ICASSP 2023 - 2023 IEEE International Conference on Acoustics, Speech and Signal Processing (ICASSP) | 978-1-7281-6327-7/23/$31.00 ©2023 IEEE | DOI: 10.1109/ICASSP49357.2023.10096523

EQUIVALENCE OF APERTURE REDUCTION IN ELEMENT SPACE AND CONSTRAINED COMBINATION OF DFT BEAMS IN BEAMSPACE

Damir Rakhimov, Martin Haardt

Communications Research Laboratory, Ilmenau University of Technology,
P. O. Box 100565, D-98684 Ilmenau, Germany
Email: {damir.rakhimov, martin.haardt}@tu-ilmenau.de

ABSTRACT

In this paper, we present an analytical proof of equivalence of the signal processing in the reduced aperture element space and in beamspace produced by the combination of multiple adjacent DFT beams with a subsequent constraining of the resulting magnitudes. This link finds applications in millimeter wave (mmWave) communications and radars that are typically equipped with a small number of RF chains and employ hybrid beamforming with analog phase shifters. This result unifies the transceiver designs, reduces complexity, and proves the applicability of state-of-the-art beamspace-based methods. It has a special implication for channel estimation at the initial stage when terminals acquire coarse estimates of the Sectors-of-Interest (SoIs). We show that the constrained groups of beams are equivalent to DFT beamformers of a smaller size aperture and present a closed-form expression of the corresponding effective aperture length as a function of the number of beams. We also derive an approximation of this expression to find the indices of the active array elements in a closed form. Finally, we verify this theory and analyze the accuracy of the proposed approximation using numerical simulations.

***Index Terms*—** Hybrid beamforming, DFT beampace, aperture reduction, constrained combination of DFT beams

1. INTRODUCTION

Hybrid beamforming architectures [1], [2] are characterized by a relatively small number of digital branches (or RF chains) which are connected to a large number of antennas via a network of analog phase shifters. Such an analog part can be seen as a beamspace transformation block that projects the input signals at the antennas to a lower dimensional space of RF chains. This is the reason why beamspace algorithms have become a common approach for signal processing at mmWave frequencies [1], [2]. At the same time, many hybrid beamforming algorithms for the mmWave frequency range require prior information about the spatial locations of the dominant paths for proper operation. Different well-known subspace-based high-resolution parameter estimation techniques such as Beamspace MUSIC [3], Beamspace ESPRIT [4], including the recently proposed R-D Unitary Tensor ESPRIT in DFT beamspace [5] can be applied to solve this task.

This work is a result of our investigations on methods for initial (coarse) channel estimation for wireless communications and radars operating in the millimeter wave frequency range. In [5] we have proposed a two-step channel estimation algorithm to obtain accurate information about the parameters of dominant multipath components. However, the current implementation requires two different algorithms which increases the complexity of the proposed solution. The link presented in this paper allows us to replace R-D Tensor-ESPRIT in element space by R-D Tensor-ESPRIT in DFT beamspace in [5] because we can consider the aperture reduction as an operation that makes the DFT beams wider without changing their shape. As a result, we can reduce the hardware complexity and unify the design of the channel estimation module for the mmWave transceiver.

In this paper, we present a link between the aperture reduction in element space and the combination of multiple adjacent DFT beams with the subsequent projection of the resulting amplitudes in the beamspace. We analytically prove this link, present the derivation of it, and show the expression for the indices of the active antenna elements after projection. Moreover, we present a closed-form expression of the effective aperture length as a function of the number of beams.

In this paper, we follow the same notation as in [5].

2. SYSTEM MODEL

In this investigation, we focus only on uniform linear arrays at the receiver side with M antennas. However, the presented results can be extended to the transmitter side and to different array configurations, for example, to uniform rectangular arrays. Without loss of generality, we also assume that M is an even number. The spacing between elements is equal to Δ. We define the aperture length normalized by the inter-element spacing of the linear array as $A = M$. The array steering vector $\boldsymbol{a}(\mu) \in \mathbb{C}^{M\times 1}$ is defined as

$$\boldsymbol{a}(\mu) = \alpha(\mu) \cdot \mathrm{e}^{-j\left(\frac{M-1}{2}\right)\mu} \cdot \begin{bmatrix} 1 & \mathrm{e}^{j\mu} & \cdots & \mathrm{e}^{j(M-1)\mu} \end{bmatrix}^{\mathrm{T}}, \quad (1)$$

where $\mu(\theta) = -\frac{2\pi}{\lambda}\Delta\sin(\theta)$ is the spacial frequency, while θ is the corresponding angle of arrival (AoA), $\alpha(\mu)$ represents the complex response of each antenna element as a function of the spatial frequency μ. Further, we assume $\alpha(\mu) = 1$. We choose the phase center of the antenna array to be in the middle of the array aperture.

For the beamforming vector, we use the phase-shifted columns of a DFT matrix. The column $\boldsymbol{w}_k \in \mathbb{C}^{M\times 1}$ is defined as

$$\begin{aligned}\boldsymbol{w}_k &= \left[\; w_k^{(0)} \;\; \cdots \;\; w_k^{(m)} \;\; \cdots \;\; w_k^{(M-1)} \;\right]^{\mathrm{T}} \\ &= \mathrm{e}^{-j\left(\frac{M-1}{2}\right)\gamma_k} \cdot \left[\; 1 \;\; \mathrm{e}^{j\gamma_k} \;\; \mathrm{e}^{j2\gamma_k} \;\; \cdots \;\; \mathrm{e}^{j(M-1)\gamma_k} \;\right]^{\mathrm{T}}, \quad (2)\end{aligned}$$

where $\gamma_k = k\frac{2\pi}{M}$, $k \in \{0, 1, \ldots, M-1\}$ is the phase increment between two adjacent antenna elements that corresponds to the spatial frequency of the pointing direction [6].

The DFT beamspace manifold for the k-th beam can be expressed as $b_k(\mu) = \boldsymbol{w}_k^{\mathrm{H}}\boldsymbol{a}(\mu)$, which after inserting the definition of the steering vector $\boldsymbol{a}(\mu)$ and the beamforming vector $\boldsymbol{w}_k$ can be written as in [6]

$$b_k(\mu) = \mathrm{e}^{-j\left(\frac{M-1}{2}\right)(\mu-\gamma_k)} \cdot \sum_{m=0}^{M-1} \mathrm{e}^{jm(\mu-\gamma_k)}. \quad (3)$$

Then we can simplify the expression (3) by applying the summation rule for the geometric progression $S_M = \frac{q^M-1}{q-1}$ and taking into account that $\frac{\mathrm{e}^{j\alpha}-\mathrm{e}^{-j\alpha}}{2j} = \sin(\alpha)$ as

$$b_k(\mu) = \frac{\mathrm{e}^{-j\frac{M}{2}(\mu-\gamma_k)}}{\mathrm{e}^{-j\frac{1}{2}(\mu-\gamma_k)}} \cdot \frac{\mathrm{e}^{jM(\mu-\gamma_k)}-1}{\mathrm{e}^{j(\mu-\gamma_k)}-1} = \frac{\sin\left(\frac{M}{2}(\mu-\gamma_k)\right)}{\sin\left(\frac{1}{2}(\mu-\gamma_k)\right)}. \quad (4)$$

3. EQUIVALENCE FORMULATION

In this section, we derive a closed-form expression of the effective aperture length as a function of the number of beams.

First, we consider the average[1] the corresponding weights for two consecutive DFT beams. We start with evaluating the amplitudes of the beamforming vector and then analyze the resulting beam pattern.

For two beamforming vectors $\boldsymbol{w}_k$ and $\boldsymbol{w}_{k+1}$, the resulting amplitude $w_{\mathrm{c}}^{(m)}$ at the antenna element with the index m can be written as

$$\begin{aligned}w_{\mathrm{c},k+\frac{1}{2}}^{(m)} &= \frac{1}{2}\left(w_k^{(m)} + w_{k+1}^{(m)}\right) \\ &= \mathrm{e}^{j\left(m-\frac{M-1}{2}\right)\gamma_{k+\frac{1}{2}}} \cdot \cos\left[\left(m - \frac{M-1}{2}\right)\frac{\pi}{M}\right], \quad (5)\end{aligned}$$

where we used $\gamma_{k+\frac{1}{2}} = \left(k+\frac{1}{2}\right)\frac{2\pi}{M}$ and the property $\frac{\mathrm{e}^{j\alpha}+\mathrm{e}^{-j\alpha}}{2} = \cos(\alpha)$.

[1]Averaging instead of summation ensures that the magnitudes of the resulting coefficients will be within the range $[0, 1]$.

As we can see from expression (5), the resulting beam is pointing in the direction between the two beams $\left(k+\frac{1}{2}\right)\frac{2\pi}{M}$ while the change in the magnitude over the array aperture is determined by the cosine function that has the largest value near the middle of the aperture $\cos\left(\frac{1}{M}\cdot\frac{\pi}{2}\right) \approx 1$ and the lowest values at the edges $\cos\left(\frac{M-1}{M}\cdot\frac{\pi}{2}\right) \approx 0$ for an even value of M.

Then we round the resulting amplitudes to the closest integer value (0 or 1) to perform the projection onto a finite set of allowable values. We can find the indices of the active antenna elements with the unit amplitude if we consider the amplitude of the expression (5)

$$\cos\left[\left(m - \frac{M-1}{2}\right)\frac{\pi}{M}\right] \geq \frac{1}{2}. \quad (6)$$

From where we can get the argument as

$$\begin{aligned}-\frac{\pi}{3} \leq &\left[\left(m - \frac{M-1}{2}\right)\frac{\pi}{M}\right] \leq \frac{\pi}{3}, \\ \frac{M-1}{2} - \frac{M}{3} \leq &\, m \leq \frac{M-1}{2} + \frac{M}{3}. \quad (7)\end{aligned}$$

The expression (7) allows us to find the indices of active array elements to broaden the resulting beamforming vector and satisfy constraints imposed on the beamforming amplitudes.

It can also be shown that the resulting beam pattern as a function of the direction of arrival might be found as

$$\begin{aligned}b_{\mathrm{cp},k+\frac{1}{2}}(\mu) &= \mathrm{e}^{-j\left(\frac{M-1}{2}\right)\left(\mu-\gamma_{k+\frac{1}{2}}\right)} \cdot \sum_{m=\lceil\frac{M-3}{6}\rceil}^{\lfloor\frac{5M-3}{6}\rfloor} \mathrm{e}^{jm\left(\mu-\gamma_{k+\frac{1}{2}}\right)} \\ &\approx \frac{\sin\left(\frac{\frac{2}{3}M}{2}\left(\mu-\gamma_{k+\frac{1}{2}}\right)\right)}{\sin\left(\frac{1}{2}\left(\mu-\gamma_{k+\frac{1}{2}}\right)\right)}. \quad (8)\end{aligned}$$

For large values of M the expression in (8) can be treated as an exact one rather than as an approximation. As a result, we can see that this projection leads to the DFT-shaped beams but with an increased angular width of the resulting mainlobe in the far-field.

Moreover, it can be observed that for large M the lower bound of the effective normalized aperture for the constrained combination of two beams is equal to
$A^{(\mathrm{eff})}(B=2; M) = \left\lfloor\frac{2}{3}M\right\rfloor$.

Following the same procedure, we can show that the indices of the active antenna elements in case of taking the average of three consecutive beams can be found as

$$\frac{M-1}{2} - \frac{M}{2\pi}\cos^{-1}\left(\frac{1}{4}\right) \leq m \leq \frac{M-1}{2} + \frac{M}{2\pi}\cos^{-1}\left(\frac{1}{4}\right). \quad (9)$$

The lower bound of the length of the resulting effective normalized aperture in this case is equal to

$$A^{(\mathrm{eff})}(B=3; M) = \left\lfloor\frac{2\cdot\cos^{-1}\left(\frac{1}{4}\right)}{2\pi}M\right\rfloor \approx \left\lfloor\frac{5}{12}M\right\rfloor. \quad (10)$$

Next, we show that the m-th element of the resulting vector $\boldsymbol{w}_{\mathrm{c}}$ after the summation over B consecutive beams can be written as

$$w_{\mathrm{c},k+\frac{B-1}{2}}^{(m)} = \frac{1}{B}\cdot\sum_{l=0}^{B-1} w_{k+l}^{(m)} = \frac{1}{B}\cdot\sum_{l=0}^{B-1} \mathrm{e}^{j\left(m-\frac{M-1}{2}\right)(k+l)\frac{2\pi}{M}}$$
$$=\frac{1}{B}\cdot \mathrm{e}^{j\left(m-\frac{M-1}{2}\right)\frac{2\pi}{M}k}\cdot\sum_{l=0}^{B-1}\mathrm{e}^{j\left(m-\frac{M-1}{2}\right)\frac{2\pi}{M}l}, \quad (11)$$

which by applying the same properties that we used to simplify the expression (3) leads to

$$\mathrm{e}^{j\left(m-\frac{M-1}{2}\right)\left(k+\frac{B-1}{2}\right)\frac{2\pi}{M}}\cdot\frac{\sin\left[\left(m-\frac{M-1}{2}\right)\frac{\pi}{M}B\right]}{B\sin\left[\left(m-\frac{M-1}{2}\right)\frac{\pi}{M}\right]}. \quad (12)$$

The resulting beam is pointing in the direction of the center of the group of B beams with the corresponding spatial frequency of $\left(k+\frac{B-1}{2}\right)\frac{2\pi}{M}$, while the amplitudes over different array elements are defined by the second term of the expression (12).

After that, we turn to find the general expression for the active elements of the array after constraining the resulting magnitude. To this end, we need to find such indices m that will satisfy the following expression

$$\frac{\sin\left[\left(m-\frac{M-1}{2}\right)\frac{\pi}{M}B\right]}{B\sin\left[\left(m-\frac{M-1}{2}\right)\frac{\pi}{M}\right]} \geq \frac{1}{2}. \quad (13)$$

The expression (13) has no analytical solution and might be solved only approximately. However, we show that the accuracy of this approximation is sufficient for practical applications.

For small values of the argument, i.e., when M is large, one can approximate the expression by a $\mathrm{si}\,()$ function

$$\frac{\sin(\alpha x)}{\alpha\sin(x)} \approx \frac{\sin(\alpha x)}{\alpha x} = \mathrm{si}\,(\alpha x) \stackrel{!}{=} \frac{1}{2}, \quad (14)$$

which we can further approximate using the first three components of the Taylor series

$$\mathrm{si}\,(\alpha x) \approx 1 - \frac{(\alpha x)^2}{3!} + \frac{(\alpha x)^4}{5!} \stackrel{!}{=} \frac{1}{2} \quad (15)$$

for the range of the main lobe of the $\mathrm{si}\,()$ function. We are interested in the solutions of the expression (15) that are close to the origin. They can be found analytically by solving the equation (15) of the 4-th order and are equal to

$$x = \pm\frac{\sqrt{10-\sqrt{40}}}{\alpha} = \pm\frac{\psi_0}{\alpha} \approx \pm\frac{2}{\alpha}, \quad (16)$$

where $\psi_0 = \sqrt{10-\sqrt{40}}$.

Using the approximation (14) and the solution (16) we can find the indices of the active antenna elements in (13) for the combination of B beams as

$$-\psi_0 \leq \left(m-\frac{M-1}{2}\right)\frac{\pi}{M}B \leq \psi_0,$$
$$\frac{M-1}{2} - \psi_0\frac{M}{\pi B} \leq m \leq \frac{M-1}{2} + \psi_0\frac{M}{\pi B}, \quad (17)$$

while the corresponding general expression for the lower bound of the effective normalized aperture length is equal to

$$A^{(\mathrm{eff})}(B;M) \approx \left\lfloor \frac{2\,\psi_0}{\pi\,B}M \right\rfloor. \quad (18)$$

The resulting beam pattern for B consecutive DFT beams after projection onto the weights $\{0,1\}$ can be written as

$$b_{\mathrm{cp},k'}(\mu) \approx \frac{\sin\left(\frac{M'}{2}(\mu-\gamma_{k'})\right)}{\sin\left(\frac{1}{2}(\mu-\gamma_{k'})\right)}, \quad (19)$$

where $k' = k + \frac{B-1}{2}$ is the spatial center of the resulting beam and $M' = \frac{2\,\psi_0}{\pi\,B}M$ is the effective size of the normalized aperture after projection.

We should keep in mind that the resulting expression (17) for the indices is based on the approximation (14) that is valid only for large values M and B. As a result, for $B = \{2,3\}$ this expression might lead to inaccurate results. Thus, for relatively small groups of beams, it is better to use the expressions (7) for the combinations of two beams and (9) in the case of three beams.

4. SIMULATION RESULTS

In this part, we present selected simulation results to illustrate the obtained analytical expressions. The simulations are obtained via a numerical evaluation of the beampattern in the far-field of the antenna array and a numerical analysis of the target parameters. For the simulation setup, we consider a uniform linear array with $M = 64$ elements and inter-element spacing $\Delta = \lambda/2$.

The comparison of the amplitude distribution for the original and the reduced apertures can be observed in Fig. 1(a) and 1(d). In Fig. 1(a) we show two consecutive DFT beams $k = \{0,1\}$ in gray color. The combination of two beams without any restriction on magnitude is given in red color. The constrained combination of the two beams is shown in blue color. We can observe that the resulting beampattern has the same shape as the original DFT beams but with a wider width of the main lobe and a similar level of side lobes with respect to the maximum gain. Thus we can conclude that it corresponds to a smaller array aperture. Similar results can be observed for the case when $B = 3$, $k = \{0,1,2\}$ in the Fig. 1(d), where the resulting beam has an even wider main lobe.

The resulting constrained combination of beams (blue curves in Fig. 1(a), 1(d) have the same level of sidelobes $\approx -13\,\mathrm{dB}$ as the original DFT beams (grey curves in

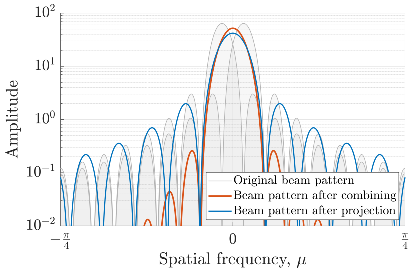

(a) Beamspace manifolds for $B = 2$.

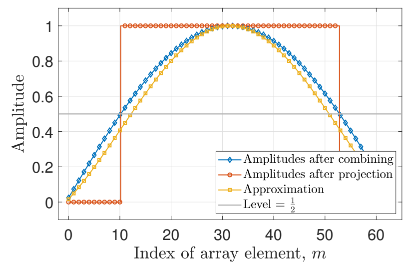

(b) Amplitudes over the aperture for $B = 2$.

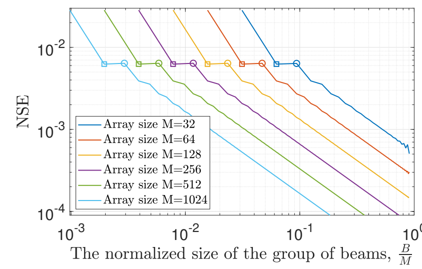

(c) NSE as function of the normalized size of the group of beams $\frac{B}{M}$.

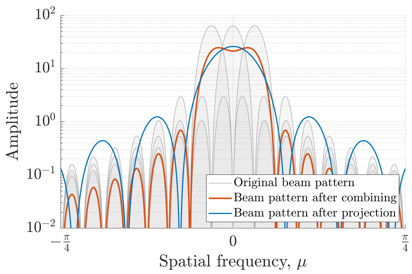

(d) Beamspace manifolds for $B = 3$.

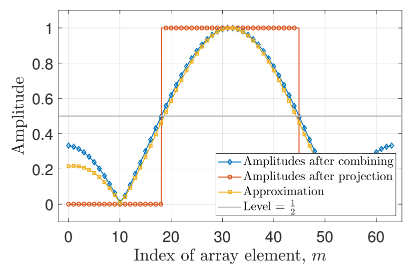

(e) Amplitudes over the aperture for $B = 3$.

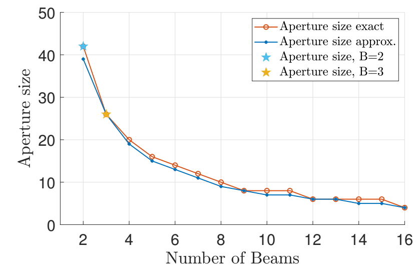

(f) Aperture size as a function of the number of beams in a group B.

Fig. 1. Numerical results and accuracy analysis.

Fig. 1(a), 1(d)). However, the gain of the resulting beam will be lower due to the smaller size of the corresponding apertures. Using the conventional analysis of antenna arrays [7], we can show that the level of the first sidelobes for the unconstrained combination of beams (red curves in Fig. 1(a), 1(d)) is reduced with an increase of the number of beams B and can be approximated by

$$\mathrm{SLL}_{\mathrm{dB}} \approx 20 \log_{10} \left| \frac{2}{\pi} \sum_{n=1}^{B} \frac{(-1)^n}{1+2n} \right|. \tag{20}$$

However, it comes at the cost of varying amplitudes at different antennas.

The amplitude weights across the aperture of the array are shown in Fig. 1(b) for $B = 2$ and in Fig. 1(e) for $B = 3$. The blue lines on these figures correspond to amplitudes for $B = 2$, and for $B = 3$. The yellow line corresponds to the approximation based on (14). The red line shows the magnitude over the aperture of the array after the projection onto the set of weights. The grey line represents the level $\frac{1}{2}$.

The approximation error of the expression in (14) is shown in Fig. 1(c). The approximation error is shown in terms of the normalized squared error (NSE), which is calculated using the expression

$$\mathrm{NSE} = \frac{|x - x_{\mathrm{approx}}|^2}{|x|^2}. \tag{21}$$

For each curve, two special points are marked that correspond to the beam groups $B = 2$ (square marker), $B = 3$ (circle marker), where the NSE has an abnormal behavior. We can see from the Fig. 1(c) that the approximation error for (14) decreases exponentially with an increase of the number of beams B in the group.

For the results depicted in Fig. 1(f), we compare the resulting aperture for different sizes of groups of beams with the approximation in (18). The red line corresponds to the exact aperture size obtained by numerical evaluation. The blue line is the lower bound on the aperture size provided by the expression in (18). The blue and yellow stars correspond to the analytical expressions on the aperture size for the cases when $B = 2$ and $B = 3$. As we can see, they match the aperture size obtained via numerical simulations.

5. CONCLUSION

In this paper, we present a link between amplitude-constrained combinations of DFT beams in beamspace and aperture reduction in element space. This result can be applied to switch signal processing from element space to beamspace for applications involving uniform linear arrays. This is, for example, the case for communications and radars operating in the mmWave frequency range when only a limited number of RF chains is available, as described in [5]. We prove this link analytically and derive a general expression for the indices of active sensors. The presented simulation results confirm this derivation and show the accuracy of the proposed closed-form expression of the effective aperture length as a function of the number of beams. These results facilitate the development of transceivers and radars for the mmWave frequency range via a unification of the design and a reduction of the complexity.

6. REFERENCES

[1] Robert W. Heath, Nuria Gonzalez-Prelcic, Sundeep Rangan, Wonil Roh, and Akbar M. Sayeed, "An Overview of Signal Processing Techniques for Millimeter Wave MIMO Systems," *IEEE Journal of Selected Topics in Signal Processing*, vol. 10, no. 3, pp. 436–453, 2016.

[2] Jun Zhang, Xianghao Yu, and Khaled B. Letaief, "Hybrid Beamforming for 5G and Beyond Millimeter-Wave Systems: A Holistic View," *IEEE Open Journal of the Communications Society*, vol. 1, pp. 77–91, 2020.

[3] Michael D. Zoltowski, Gregory M. Kautz, and Seth D. Silverstein, "Beamspace Root-MUSIC," *IEEE Transactions on Signal Processing*, vol. 41, no. 1, pp. 344, 1993.

[4] Guanghan Xu, Seth D. Silverstein, Richard H. Roy, and Thomas Kailath, "Beamspace ESPRIT," *IEEE Transactions on Signal Processing*, vol. 42, no. 2, pp. 349–356, 1994.

[5] Jianshu Zhang, Damir Rakhimov, and Martin Haardt, "Gridless Channel Estimation for Hybrid mmWave MIMO Systems via Tensor-ESPRIT Algorithms in DFT Beamspace," *IEEE Journal of Selected Topics in Signal Processing*, vol. 15, no. 3, pp. 816–831, 2021.

[6] Michael D. Zoltowski, Martin Haardt, and Cherian P. Mathews, "Closed-form 2-D angle estimation with rectangular arrays in element space or beamspace via unitary ESPRIT," *IEEE Transactions on Signal Processing*, vol. 44, no. 2, pp. 316–328, 1996.

[7] Constantine A. Balanis, *Antenna theory: Analysis and design*, Wiley, Hoboken, New Jersey, fourth edition, 2016.